Peptide Adsorption and Assembly

DOI: 10.1002/anie.200805259

Adsorption, Diffusion, and Self-Assembly of an Engineered Gold-Binding Peptide on Au(111) Investigated by Atomic Force Microscopy**

*Christopher R. So, Candan Tamerler, and Mehmet Sarikaya**

There is a growing interest in using peptides that bind to inorganic solids as molecular building blocks in nanotechnology and in medicine, mainly owing to their material-selective properties.[1] These short peptides (7–14 amino acids long), which are identified by biocombinatorial selection procedures, are utilized as reducing agents in the synthesis of inorganic materials, molecular erectors, and probes when genetically fused to other functional proteins and enzymes[1,2] or to molecular assemblers[1,3] and when coupled with nanoparticles and quantum dots for targeted organization of hybrid functional nanostructures.[1–4] Despite the growing list of newly discovered solid-binding peptides and their increased utility, there is still only a limited understanding of the mechanisms of molecular binding on solid surfaces.[5] Herein we report a quantitative atomic force microscopy (AFM) study of the adsorption of a gold-binding peptide on an atomically flat (111)-oriented gold surface and the evolution of non-equilibrium surface structures that lead to the formation of a confluent monolayer. These experimental observations and their interpretation offer new insights into the fundamental understanding of nanometer-thick peptide molecular film formation on inorganic solid surfaces.

Gold-binding peptides (GBPs) were originally selected by cell-surface display using random peptide libraries expressed on the outer surface of *E. coli* as part of the maltodextrin porin, *LamB* protein.[6] Among those identified, we use GBP_1 (MHGKTQATSGTIQS), which exhibits enhanced binding affinity when triply repeated in tandem ($3rGBP_1$; Supporting Information, Figure S1). This motif is cysteine-free and interacts with gold surfaces by mechanisms unlike conventional chemisorptive thiol–gold systems.[7] The stability of the peptide on the surface may originate from the close contact of the polar[8] (e.g., glutamine, serine, or threonine) and cationic[9] (e.g., lysine or histidine) side chains, in alignment with the underlying gold lattice. The understanding of molecular recognition of a solid surface by a peptide requires studying not only the peptide's conformation in solution but also its intermolecular interaction across the shared surface.[10] Based on Langmuir adsorption kinetics,[11,12] which can directly yield an equilibrium kinetic constant and free energy (see the Supporting Information), we first studied the effect of concentration on the observed equilibrium surface coverage of the final bound states of $3rGBP_1$. From reported surface plasmon resonance (SPR) and quartz crystal microbalance (QCM) experiments,[13] concentrations of $3rGBP_1$ achieve equilibrium within 1200 seconds of the start from the assembly process. Consequently, the AFM images in Figure 1 A a–h represent coverage states of the $3rGBP_1$ peptide film at seven different concentrations ranging from 2–2320 nM exposed over this time period. As a result, the surface exhibits variably sized structural features throughout the entire concentration regime, the dimensions of which can be quantified for coverage analysis.

Surface interactions with proteins with sizes of at least 5 nm (the resolution limit of non-contact-mode AFM) can be directly observed spatially and temporally to gain insight into the dynamics of adsorption phenomena.[14,15] Among the few other techniques available for determining quantitative single-molecule adsorption,[16] direct imaging of the surface described herein permits the observation and modeling of interactions between multiple molecules on a solid surface over long time scales. Having dimensions of a few nanometers, $3rGBP_1$ can be observed discretely as well as in aggregation in the tens-of-nanometers size regime. Owing to the large-grained nature of the evaporated Au(111) textured surface, atomically flat regions of approximately 200 nm diameter can be isolated and analyzed individually for bound surface coverage (see the Experimental Section). Figure 1 B plots various concentrations versus peptide coverage on the surface (θ), where each point in the plot was averaged over nine grains across each sample. The coverage data suggest that, under equilibrium conditions, $3rGBP_1$ appears to obey simple Langmuir adsorption.[11] This observation agrees with previous surface coverage trends obtained using SPR[13] and yields a equilibrium constant $K_{eq} = 1.41 \times 10^7\,M^{-1}$ and a corresponding change in free energy $\Delta G = -9.61\ kJ\,mol^{-1}$. Also shown in Figure 1 B is a comparison to concurrently performed SPR analysis under similar equilibrium conditions, with $K_{eq} = 0.91 \times 10^7\,M^{-1}$ and $\Delta G = -9.35\ kJ\,mol^{-1}$, supporting the trends detected here by AFM. We further investigated the adsorption process by monitoring time-dependent peptide self-assembly. On the basis of the results in Figure 1, we chose a single concentration of peptide and performed experiments to examine the structural evolution of molecular adsorption on the solid surface (Figure 2 A a–j). For reproducibility, four separate experiments were performed and quantified at

[*] C. R. So, Prof. C. Tamerler, Prof. M. Sarikaya
MSE; Genetically Engineered Materials Science and Engineering Center, University of Washington
302 Roberts Hall, Seattle, WA 98195 (USA)

[**] This research was supported fully by the National Science Foundation through the MRSEC program. We thank U. O. Seker and B. Wilson for their assistance, discussions, and input.

Supporting information for this article is available on the WWW under http://dx.doi.org/10.1002/anie.200805259.

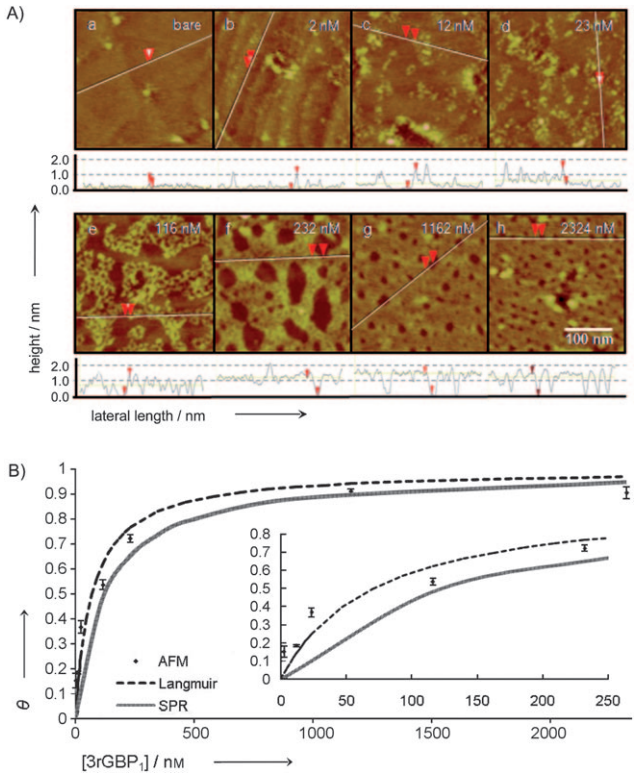

Figure 1. A) Concentration-dependent AFM images (a–h) of the Au(111) substrate exposed to 3rGBP$_1$ solution for 1200 s with corresponding cross-sectional height profiles. The scale is the same for images (a–h). The white lines show the trajectory of the height profiles, and the arrows in the AFM images correspond to those in the height profiles beneath. B) Corresponding isotherm plot of 3rGBP$_1$ surface coverage on gold. Error bars represent ±1 standard deviation of in-sample variation. A least-squares-error curve fit to Equation (S3-4) in the Supporting Information was used to generate the Langmuir plot. The inset is an enlargement of the plot for 0–250 nM.

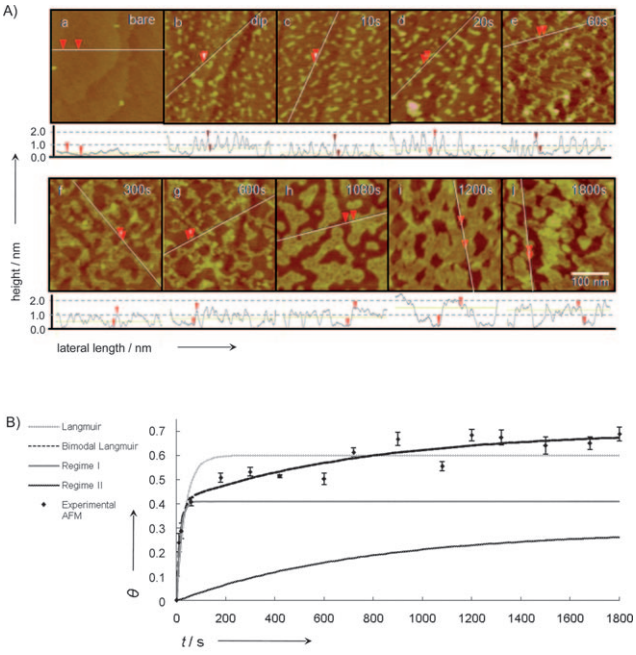

Figure 2. A) AFM images, with cross-sectional heights, of time-dependent adsorption states of 3rGBP$_1$ on Au(111) showing initial discrete monomeric and clustered states (b), elongated cluster states (c–e), and percolated monolayer states (f–j). The scale is the same for images (a–j). The white lines show the trajectory of the height profiles, and the arrows in the AFM images correspond to those in the height profiles beneath. B) Surface coverage plot of 3rGBP$_1$ adsorption on Au(111) over time with a bulk concentration of 232 nM. Least-square-error curve fit to Equation (S3-5) in the Supporting Information was used to generate the Langmuir plot.

various timescales to attain the composite adsorption curve shown in Figure 2B. The concentration-dependent adsorption (Figure 1) suggests that the observed equilibrium states obey a Langmuir-type behavior. However, the time-dependent adsorption of the peptides shown in Figure 2B is significantly more complex. Over time, the adsorbed peptide forms structures that vary from initial homodisperse monomers to branch-like nanostructures, eventually forming a percolated film on the (111) gold surface. As shown in Figure 2B, two distinct modes of coverage kinetics are observed simultaneously, leading to a dual morphological growth process. These surface-coverage trends are best fit by a two-domain Langmuir model similar to the observations by Tamerler.[13] This analysis gives a least-squares correlation value of 0.926 in comparison to that of 0.862 from the single-domain equation, that is, the time-dependent Langmuir model as indicated in Figure 2B.

The phenomenon of two-stage assembly kinetics may be explained by more rigorous analysis of the observations. The faster process, termed regime I, occurs rapidly during the initial stages involving homogeneous monomer adsorption across the solid surface (ca. 10 islands per 100 nm^2), which is followed immediately by aggregation and growth into small elongated clusters. Throughout early adsorption, competition occurs between these two predominant surface morphologies. The adsorption–aggregation processes last for at least 60 seconds, until the clusters percolate and are sterically hindered from further growth (Figure 2A b–e). The perceived monomers, about 5–10 nm in diameter (including AFM tip convolution), are most likely single peptides, or possibly dimers, based on dimensions of 3rGBP$_1$ established by solution-state NMR spectroscopy (i.e., 1 nm × 2 nm × 4 nm).[9] The elongated clusters appear dominant and remain so through the early adsorption process; they are distinguished from monomers and classified as "nuclei" for diffusion coefficient calculations (see the Supporting Information). From Figure 2A a–e, analyzed in Figure 3A, the number density of monomers relative to nuclei decreases dramatically, while the average feature-size distribution broadens over time (Figure 3B). The nuclei, therefore, grow at the expense of monomers through a rapid coalescence resulting in coverage increase. This process suggests that significant peptide mobility and intermolecular interactions occur across the gold surface. The accompanying processes result in an overall coverage growth rate of approximately 4×10^{-3} cm^2 s^{-1}. Interestingly, the apparent nucleation and growth mechanisms can be accurately described using structure-based rate equations developed for the evolution of

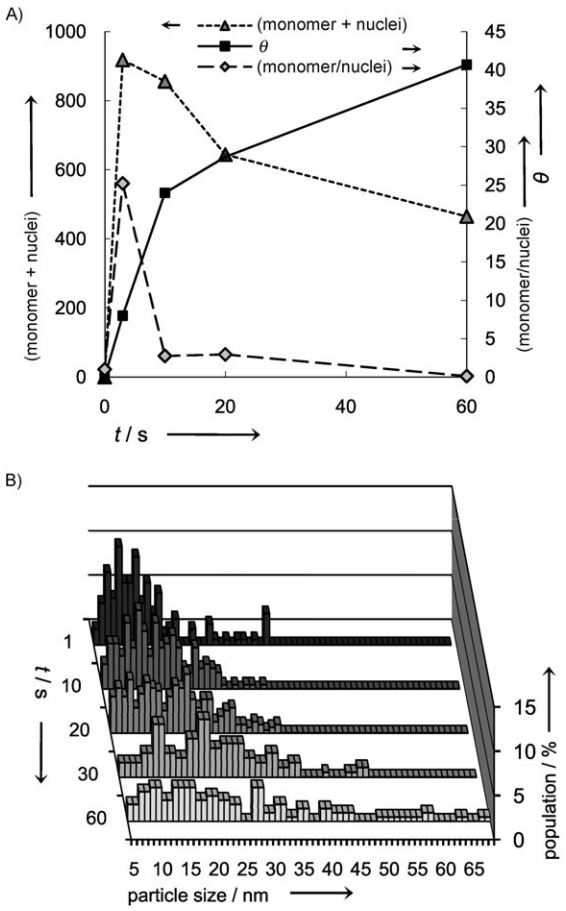

Figure 3. A) Quantification of total feature density, monomer/nuclei ratio, and percent coverage over time showing nuclei growing at the expense of monomers. B) Particle-size analysis of the first 60 seconds of adsorption normalized to percent population, showing significant peak broadening as an indication of peptide surface diffusion. All data is collected over 1 μm^2.

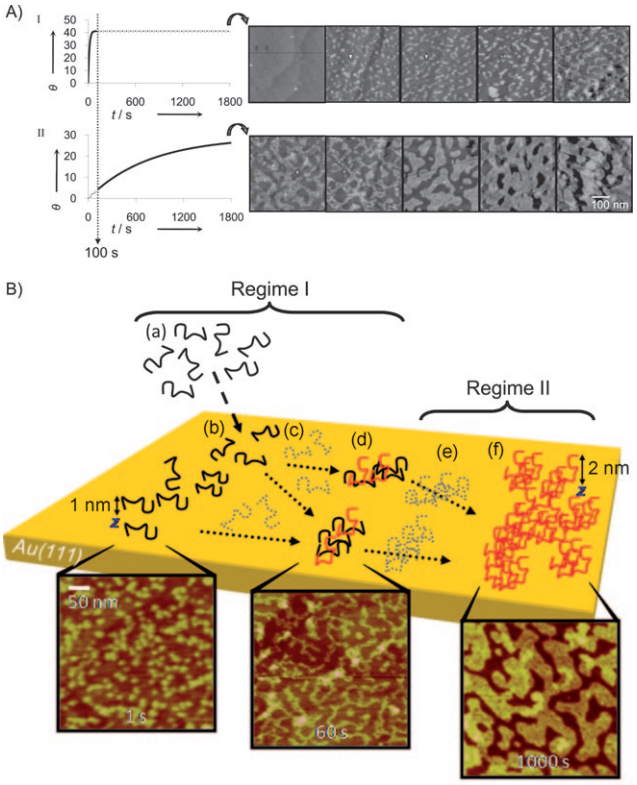

Figure 4. A) Deconstruction of the two-domain Langmuir curve into regime I and regime II, associated with the corresponding AFM images. B) Schematic model showing the proposed mechanism of the binding, diffusion, and assembly of 3rGBP$_1$ on Au(111) with corresponding AFM images and identification of growth regimes I and II. See text for details.

nanostructures in atomic and molecular thin-film deposition of metals.[17] From monomer adsorption and nucleation during regime I, we calculate the surface diffusion rate for a peptide monomer to be about 1×10^{-12} $cm^2 s^{-1}$ after applying the mean-field nucleation theory (see the Supporting Information).

During regime II, the second stage of the growth process, the percolated network of peptides forms a scaffold which slowly ripens at a rate (10^{-4} $cm^2 s^{-1}$) an order of magnitude slower than for regime I. This finding suggests that an entirely different assembly mechanism dominates the later stages of peptide film formation. From Figure 2B, regime II remains initially insignificant and only contributes 5% to the overall surface coverage during the initial 100 seconds; however, it eventually contributes approximately 40% total coverage throughout the rest of the adsorption process. We conclude that "regime I" is represented in Figure 2A a–e and "regime II" in Figure 2A f–j, as summarized in Figure 4A. The morphology at times longer than 1200 seconds remains virtually unchanged, reflecting the state of kinetic equilibrium achieved by the peptide film on the solid surface with a persistent coverage of approximately 67%. When compared to the previous concentration-dependent Langmuir behavior (Figure 1B), this equilibrium coverage falls well within the expected value.

Figure 4B schematically depicts a model for understanding peptide interaction with an atomically flat solid in solution. In this model, six stages of peptide–solid interactions are considered in a system exposed to a fixed concentration of peptide. In regime I (Figure 4B a–d), peptides bind as monomers to the solid surface and undergo surface diffusion to form nuclei that are highly mobile and coalesce to reach a critical length (50–100 nm), resulting in a percolated, branched network. During regime II (Figure 4B e,f), the network undergoes slow ripening and captures newly adsorbed monomers to fill out the remaining interstitial space on the surface. We therefore attribute the bimodal Langmuir behavior, seen in AFM as well as SPR (Supporting Information, Figure S2), to the surface diffusion of 3rGBP$_1$ and its aggregation to form a molecular thin film on gold.

In summary, we show herein for the first time a morphological basis for the binding and assembly of an engineered peptide, which arises from its specific interaction with a solid surface. The adsorption process of the gold-binding peptide on Au(111) is dynamic and involves multiple stages of structure evolution over time with accompanying surface diffusivities. The observed structures of adsorbed peptides are explained by well-established theories of sub-

monolayer nucleation and island growth developed for metallic and semiconductor heterostructures, the basis of today's microelectronic and magnetic thin films.[15,17] Analogous to molecular recognition among biological proteins,[18] which leads to specific functions, understanding the molecular recognition of solids[19] by engineered peptides, their self-assembly, and their topology is of fundamental significance, as such interactions could well form the basis of novel hybrid molecular technologies in which the immobilization of proteins, with high affinity and material selectivity, is an essential component in building up protein chips, protein microarrays, and biosensors.[20]

Received: October 27, 2008
Revised: January 14, 2009
Published online: April 6, 2009

Keywords: molecular biomimetics · monolayers · peptides · self-assembly · surface diffusion

[1] M. Sarikaya, C. Tamerler, A. K. -Y. Jens, K. Schulten, F. Baneyx, *Nat. Mater.* **2003**, *2*, 577; C. Tamerler, M. Sarikaya, *MRS Bull.* **2008**, *33*, 504; F. Baneyx, D. T. Schwartz, *Curr. Opin. Biotechnol.* **2007**, *18*, 312.
[2] S. R. Whaley, D. S. English, E. L. Hu, P. F. Barbara, A. M. Belcher, *Nature* **2000**, *405*, 665.
[3] R. R. Naik, S. J. Stringer, G. Agarwal, S. E. Jones, M. O. Stone, *Nat. Mater.* **2002**, *1*, 169; M. M. Tomczak, D. D. Glawe, L. F. Drummy, C. G. Lawrence, M. O. Stone, C. C. Perry, D. J. Pochan, T. J. Deming, R. R. Naik, *J. Am. Chem. Soc.* **2005**, *127*, 12577.
[4] H. X. Dai, W-S. Choe, C. K. Thai, M. Sarikaya, B. A. Traxler, F. Baneyx, D. T. Schwartz, *J. Am. Chem. Soc.* **2005**, *127*, 15637; M. T. Zin, H. Ma, M. Sarikaya, A. K.-Y. Jens, *Small* **2005**, *1*, 698.
[5] C. B. Mao, D. J. Solis, B. D. Reiss, T. Kottmann, R. Y. Sweeney, A. Hayhurst, G. Georgiou, B. Iverson, A. M. Belcher, *Science* **2004**, *303*, 213; A. Herman, L. Addadi, S. Weiner, *Nature* **1988**, *331*, 546; J. J. Gray, *Curr. Opin. Struct. Biol.* **2004**, *14*, 110; S. G. Zhang, *Nat. Biotechnol.* **2003**, *21*, 1171.
[6] S. Brown, M. Sarikaya, E. Johnson, *J. Mol. Biol.* **2000**, *299*, 725.
[7] R. G. Nuzzo, B. R. Zegarski, L. H. Dubois, *J. Am. Chem. Soc.* **1987**, *109*, 733.
[8] R. Braun, M. Sarikaya, K. Schulten, *J. Biomater. Sci. Polym. Ed.* **2002**, *13*, 747.
[9] J. L. Kulp III, M. Sarikaya, J. S. Evans, *J. Mater. Chem.* **2004**, *14*, 2325.
[10] M. Lingenfelder, G. Tomba, G. Costantini, L. C. Ciacchi, A. De Vita, K. Kern, *Angew. Chem.* **2007**, *119*, 4576 – 4579; *Angew. Chem. Int. Ed.* **2007**, *46*, 4492.
[11] K. Tamada, M. Hara, H. Sasabe, W. Knoll, *Langmuir* **1997**, *13*, 1558.
[12] K. A. Peterlinz, R. Georgiadis, *Langmuir* **1996**, *12*, 4731.
[13] C. Tamerler, E. E. Oren, M. Duman, E. Venkatasubramanian, M. Sarikaya, *Langmuir* **2006**, *22*, 7712.
[14] R. T. T. Gettens, Z. J. Bai, J. L. Gilbert, *J. Biomed. Mater. Res. Part A* **2005**, *72*, 246; O. Mermut, D. C. Phillips, R. L. York, K. R. McCrea, R. S. Ward, G. A. Somorjai, *J. Am. Chem. Soc.* **2006**, *128*, 3598; D. T. Kim, H. W. Blanch, C. J. Radke, *Langmuir* **2002**, *18*, 5841.
[15] P. A. Mulheran, D. Pellenc, R. A. Bennett, R. J. Green, M. Sperrin, *Phys. Rev. Lett.* **2008**, *100*, 068102.
[16] H. Lee, N. F. Scherer, P. B. Messersmith, *Proc. Natl. Acad. Sci. USA* **2006**, *103*, 12999.
[17] H. Brune, *Surf. Sci. Rep.* **1998**, *31*, 121; J. A. Venables, *Philos. Mag.* **1973**, *27*, 697; Y. W. Mo, J. Kleiner, M. B. Webb, M. G. Lagally, *Phys. Rev. Lett.* **1991**, *66*, 1998.
[18] L. Pauling, *Nature* **1974**, *248*, 769.
[19] S. Mann, *Nature* **1988**, *332*, 119.
[20] K.-y. Tomizaki, K. Usui, H. Mihara, *ChemBioChem* **2005**, *6*, 782; F. Rusmini, Z. Zhong, J. Feijen, *Biomacromolecules* **2007**, *8*, 1775.

